Published OnlineFirst February 4, 2019; DOI: 10.1158/1535-7163.MCT-18-0535

Companion Diagnostic, Pharmacogenomic, and Cancer Biomarkers

Molecular Cancer Therapeutics

Genome-Wide Sequencing of Cell-Free DNA Identifies Copy-Number Alterations That Can Be Used for Monitoring Response to Immunotherapy in Cancer Patients

Taylor J. Jensen[1], Aaron M. Goodman[2,3], Shumei Kato[2,4], Christopher K. Ellison[1], Gregory A. Daniels[2], Lisa Kim[2], Prachi Nakashe[1], Erin McCarthy[1], Amin R. Mazloom[1], Graham McLennan[1], Daniel S. Grosu[1], Mathias Ehrich[1], and Razelle Kurzrock[2]

Abstract

Inhibitors of the PD-1/PD-L1/CTLA-4 immune checkpoint pathway have revolutionized cancer treatment. Indeed, some patients with advanced, refractory malignancies achieve durable responses; however, only a subset of patients benefit, necessitating new biomarkers to predict outcome. Interrogating cell-free DNA (cfDNA) isolated from plasma (liquid biopsy) provides a promising method for monitoring response. We describe the use of low-coverage, genome-wide sequencing of cfDNA, validated extensively for noninvasive prenatal testing, to detect tumor-specific copy-number alterations, and the development of a new metric—the genome instability number (GIN)—to monitor response to these drugs. We demonstrate how the GIN can be used to discriminate clinical response from progression, differentiate progression from pseudoprogression, and identify hyperprogressive disease. Finally, we provide evidence for delayed kinetics in responses to checkpoint inhibitors relative to molecularly targeted therapies. Overall, these data demonstrate a proof of concept for using this method for monitoring treatment outcome in patients with cancer receiving immunotherapy.

Introduction

Cancer is a disease of the genome and is characterized by several types of alterations including point mutations, balanced and unbalanced chromosomal rearrangements, and copy-number alterations (CNA). Recently, researchers have described the genomic profiles of tumor tissue obtained from numerous primary and metastatic tumors (1–5). In addition, the release of cell-free DNA (cfDNA) by tumors into the bloodstream has been described for decades and has been recently leveraged in both research and clinical settings to facilitate therapy selection, identify drug resistance, and monitor treatment response (6–14). Depending on the breadth of the target genomic loci, this process, often called a liquid biopsy, is typically performed using digital PCR or ultra-deep next-generation sequencing (>8,000–10,000X raw coverage; refs. 6, 9, 10, 13, 15, 16). Although these assays are useful in guiding therapy through their detection of all types of mutations associated with cancer, cost factors currently necessitate these tests to narrow their content to alterations within a targeted region. In contrast, detection of CNAs via low-coverage, genome-wide sequencing of cfDNA has been validated for noninvasive prenatal testing (NIPT) where it has been applied clinically in over 100,000 patients (17–21). Because tumor aneuploidy (and thus the presence of CNAs) is a fundamental characteristic of cancer, this method has additionally detected CNAs in patients with either known or unknown neoplasms (22, 23). Here, we directly evaluate the utility of this method to detect and monitor CNAs in patients with known cancers.

The development of immune checkpoint inhibitors targeting PD-1, PD-L1, and CTLA-4 has transformed clinical practice. A subset of patients exhibits robust responses; however, challenges exist in identifying biomarkers that can be used to predict and/or monitor response to these drugs (24, 25). In addition, previous studies have described a link between the presence, type, and location of CNAs and response to immunotherapy in tissue samples (26, 27). Based upon this clinical need and the technology that has been developed, we sought to determine the feasibility of using cfDNA, specifically the detection of tumor-specific CNAs, as a biomarker to monitor response (currently assessed by standard RECIST imaging criteria; ref. 28) to checkpoint inhibitors in patients receiving these drugs as part of their care. Here, we present results from the first set of 44 evaluable patients.

[1]Sequenom, a Wholly Owned Subsidiary of Laboratory Corporation of America Holdings, San Diego, California. [2]Division of Hematology/Oncology, Department of Medicine, Center for Personalized Cancer Therapy, Moores Cancer Center, University of California, San Diego, San Diego, California. [3]Division of Blood and Marrow Transplantation, Department of Medicine, Moores Cancer Center, University of California, San Diego, San Diego, California. [4]Division of Precision Medicine, Department of Medicine, Moores Cancer Center, University of California, San Diego, San Diego, California.

Note: Supplementary data for this article are available at Molecular Cancer Therapeutics Online (http://mct.aacrjournals.org/).

T.J. Jensen and A.M. Goodman contributed equally to this article and are the co-first authors.

Corresponding Author: Taylor J. Jensen, Sequenom, 3595 John Hopkins Court, San Diego, CA 92121. Phone: 858-202-9275; E-mail: tjensen@sequenom.com

doi: 10.1158/1535-7163.MCT-18-0535

Published OnlineFirst February 4, 2019; DOI: 10.1158/1535-7163.MCT-18-0535

Materials and Methods

Patient selection

We prospectively enrolled 56 patients with cancer who were going to initiate treatment with an immunotherapy at UC San Diego Moores Cancer Center between September 2015 and April 2017. Patients were enrolled consecutively, and no other information was utilized for patient enrichment. Data were collected by chart and imaging review.

Patient treatment

Patients were treated with immunotherapy that included a checkpoint inhibitor per approved indication or on an experimental protocol. This study was performed, and informed-written consent was obtained from subjects in accordance with UCSD Institutional Review Board guidelines for specimen collection and data analysis (NCT02478931) and for any investigational treatments.

Sample collection and processing

Whole blood (~10 mL) was collected in Streck BCT tubes (Streck) and processed to plasma as previously described (29). Samples were deemed to be the baseline for each patient if the blood collection occurred prior to the initiation of immunotherapy treatment. If more than one sample was collected during that time, the baseline sample was the sample collected closest to the start of treatment.

cfDNA extraction

cfDNA from the plasma of each sample was extracted using a bead-based method as previously described (29).

Total cfDNA quantification

Total cfDNA yield from each plasma sample was estimated using droplet digital PCR (ddPCR) targeted to the human reverse transcriptase (hTERT) gene (chr5:1253373-1253460; hg19). For each reaction, an aliquot of extracted cfDNA (5–10 μL) was combined with the primer/probe mix for hTERT (Life Technologies) and 2x ddPCR supermix (Bio-Rad) and measured using a QX100 ddPCR system (Bio-Rad).

Sequencing library preparation

Libraries for genome-wide sequencing were created from cfDNA as previously described (30).

Genome-wide next-generation sequencing

Normalized sequencing libraries were pooled and sequenced using HiSeq2500 (Illumina) instruments as previously described (31). A mean of 34.4 million sequencing reads (~0.3X genomic coverage) were generated for each sample.

Sequencing data analysis

Sequencing data were processed as previously described (31). Briefly, sequencing reads were mapped to the human reference genome (hg19) and partitioned in to 50 kbp non-overlapping segments. Regions were selected, and data were normalized as previously performed for noninvasive detection of fetal copy-number variants (23, 32), and the resultant-normalized values were used to calculate a genome instability number (GIN). The GIN is a metric intended to capture genome-wide autosomal deviation from empirically derived euploid dosage of the genome in circulation and was developed and standardized prior to analyzing the data from this study. The GIN is a nonnegative, continuous value calculated as the absolute deviation of observed normalized sequencing read coverage from expected normalized read coverage summed across 50,034 autosomal segments. Observed normalized read coverage is defined for each genomic segment by an autosome-specific LOESS fit of the normalized data. The data can be represented as:

$$\mathrm{GIN} = \sum_{i=1}^{50034} |fit_i - exp_i|$$

where the GIN is defined as the sum across all autosomal bins, i, of the absolute deviation of LOESS fit of the normalized genomic representation of a sample, fit_i, to the expected normalized genomic representation of a sample without CNAs present, exp_i. Increasing values of GIN were observed to be indicative of increasing deviation relative to an expected normal genomic profile. Repeated sequencing and analysis of an independent cohort of 43 samples yielded reproducible GIN values (Pearson correlation coefficient > 0.99; Supplementary Fig. S6). In addition, specific CNAs were identified using methods previously described (32) to define the boundaries of the event as well as a z-score representing the deviation of the observed event from reference controls.

Statistical analysis and outcome evaluation

Clinical responses were assessed based on physician notation and radiograph review using RECIST criteria (28). Progression-free survival (PFS) was calculated by the method of Kaplan and Meier [P values by log-rank (Mantel–Cox)] test. Patients were censored at date of last follow-up for PFS, if they had not progressed. For disease status prediction using the GIN, patients were evaluated at the time point nearest +42 days relative to treatment start site. Statistical analyses were carried out using either custom scripts in an R programming language (33) or Graph-Pad Prism version 7.0.

Results

Patient characteristics

In total, CNAs were characterized in the cfDNA isolated from 255 blood samples obtained from 56 patients. Six patients were excluded from the analysis: two never started treatment and four never had a clinical response assessment before data censoring. For 6 of the remaining 50 patients, no baseline blood sample collected before the initiation of treatment was available. In total, a sample cohort of 228 distinct plasma samples obtained from 44 patients was included in this study (Fig. 1).

Patient characteristics are detailed in Table 1 and Supplementary Table S1. Eighteen different types of malignancies were present in the cohort with the most common being melanoma (18%), non–small cell lung cancer (18%), and breast cancer (9%). Thirty-eight patients (86%) had metastatic disease, whereas 6 patients (14%) had locally advanced disease. All 44 patients were treated with immunotherapy, either as monotherapy, or in combination with a targeted agent, chemotherapy, or another immunotherapeutic. All patients received an anti–PD-1/PD-L1 agent in their regimen (Table 1). The median (range) PFS was 2.8 months (0.1–18.4+; Fig. 2A).

Published OnlineFirst February 4, 2019; DOI: 10.1158/1535-7163.MCT-18-0535

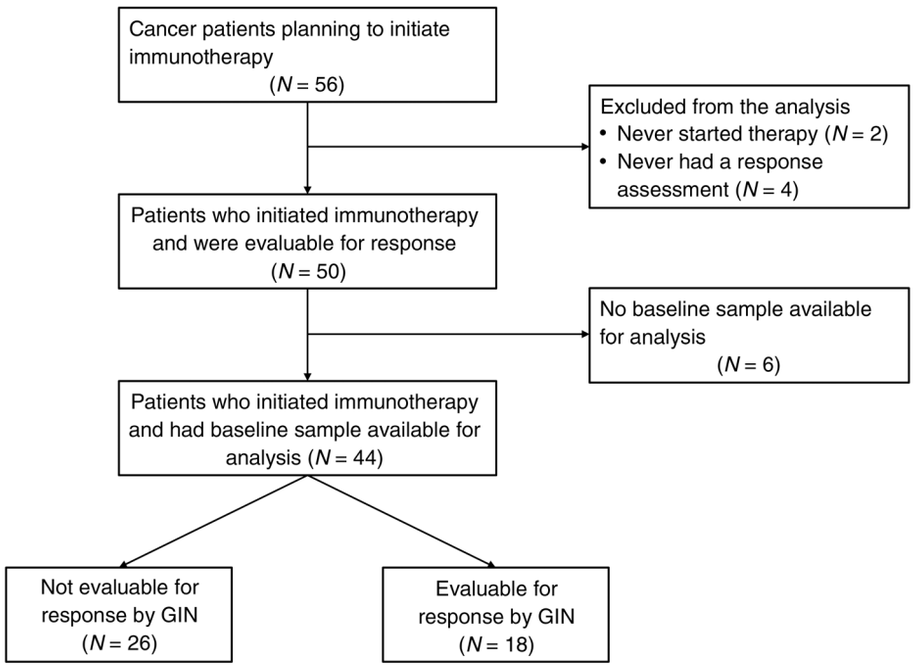

Figure 1.
CONSORT diagram of all patients included in this study. In order for a patient to be evaluable by GIN (n = 18), a sample from that patient had to have a GIN above the described threshold, and that patient needed a sufficient number of longitudinal samples for analysis.

Baseline GIN and amount of cfDNA do not correlate with immunotherapy response

A baseline sample collected before the initiation of immunotherapy treatment was characterized for each of the 44 patients. The total amount of cfDNA present in each baseline plasma sample was quantified. The amount of total cfDNA ranged from 206 to 84,012 genomic equivalents (GE) per mL of plasma with a median of 2,351 GE. To identify and quantify both the number and relative magnitude of CNAs in the cfDNA, we quantified the cumulative contribution of tumor aneuploidy and amount of circulating tumor DNA (ctDNA) in the blood by calculating the cumulative deviation of all autosomal CNAs relative to a previously defined baseline population and defined this as the GIN. The GIN within the baseline sample cohort ranged from 86 to 6,052 with a median value of 180. The GIN was also measured in an independent dataset comprised of 6,014 research-consented samples, with no detected CNAs, submitted to Sequenom Laboratories as part of standard NIPT (Supplementary Fig. S1). Because these samples were measured using the same process, they were used to estimate the technical noise of the GIN and to establish a null distribution for the value. In this independent sample cohort lacking detected CNAs (N = 6,014 samples), the GIN ranged from 56 to 162 with a median of 84. Using a threshold value of GIN >170 as positive, conservatively selected based upon the empirically derived distribution of samples without CNAs identified, CNAs were identified in 54.5% (24 of 44) of cancer patients prior to the initiation of treatment with immune checkpoint inhibitors.

Next, we evaluated whether either the GIN or the total amount of cfDNA at baseline was predictive of clinical response. Response was classified as meeting RECIST criteria for stable disease (SD) > 9 months, partial or complete clinical response (PR/CR), whereas progressive disease (PD) was designated when SD lasted $\leq$ 9 months or clinical progression was the best response noted. Out of the 44 patients, there were 13 responders, 27 progressors, and 4 patients who are not yet evaluable because they have stable disease that is ongoing for less than 9 months (Supplementary Table S1).

There was no significant difference (P = 0.48, Wilcoxon rank-sum test) in the baseline GIN between patients that ultimately showed a response to treatment (n = 13, median = 167, range = 108–5,901) versus those that showed PD (n = 27, median = 256, range = 86–6,053; Supplementary Fig. S2). Similarly, no difference was observed when comparing the total amount of cfDNA between patients that ultimately responded (median = 1,980 GE/mL plasma, range = 729–18,012) with those who did not (median = 2,791 GE/mL plasma, range = 206–84,012; Supplementary Fig. S2; P = 0.49, Wilcoxon rank-sum test). Finally, although there is a relationship between the amount of total cfDNA and the GIN in baseline samples (Spearman correlation = 0.49), additional factors likely limit the accuracy of total cfDNA alone as a marker for monitoring treatment response (Supplementary Fig. S3).

The pattern of dynamic changes in GIN after treatment predicts immunotherapy response

Although the data suggest no predictive strength of either the GIN or total cfDNA in patients prior to treatment initiation, we also evaluated whether the same analytical tools could be used to monitor the efficacy of these treatments over time. In order to predict treatment response based upon the GIN, CNAs had to be detected in the sample, and samples collected at two or more time points had to have been assayed. Based on these requirements, we were able to compare the treatment response as determined by cfDNA profiling (GIN) with RECIST imaging response criteria (28) in 18 of the 44 patients (Fig. 1). The predicted treatment response using the GIN was performed using data from about day +42 relative to treatment start or the nearest time point thereafter (unless the only time points available were earlier). Multiple plasma aliquots were collected from these patients (median, 4;

Published OnlineFirst February 4, 2019; DOI: 10.1158/1535-7163.MCT-18-0535

Table 1. Study cohort characteristics ($n = 44$)

Sex	
Men	23 (52%)
Women	21 (48%)
Median age in years (range)[a]	63 (32–89)
Ethnicity	
Caucasian	38 (86%)
Hispanic	3 (7%)
Asian	2 (5%)
Other	1 (2%)
Malignancy	
Adenoid cystic carcinoma	1 (2%)
Appendiceal carcinoma	1 (2%)
Basal cell carcinoma	2 (5%)
Bladder urothelial carcinoma	2 (5%)
Breast cancer	4 (9%)
Cervical cancer	1 (2%)
Colorectal adenocarcinoma	2 (5%)
Cutaneous squamous cell carcinoma	2 (5%)
Soft-tissue sarcoma	3 (7%)
Gastroesophageal cancer	3 (7%)
Glioblastoma	1 (2%)
Head and neck squamous cell carcinoma	1 (2%)
Hepatocellular carcinoma	2 (5%)
Melanoma	8 (18%)
Neuroendocrine tumor	1 (1%)
Non–small cell lung cancer	8 (18%)
Ovarian cancer	1 (2%)
Thyroid cancer	1 (2%)
Disease status at time of treatment and cell-free DNA collection	
Locally advanced disease	6 (14%)
Metastatic disease	38 (86%)
Treatment	
Median number of prior systemic treatments (range)	2 (0–5)
Nivolumab	16 (36%)
Pembrolizumab	19 (43%)
Atezolizumab	3 (7%)
Nivolumab + ipilimumab	3 (7%)
Nivolumab + targeted therapy	2 (5%)
Nivolumab + chemotherapy	1 (2%)
PFS in months: median (range)[b]	2.8 (0.1–18.4+)

[a]Patient's age is at the time of immunotherapy treatment and cfDNA collection.
[b]Calculated using the method of Kaplan and Meier.

range, 2–19) and used to monitor response for up to 508 days after the initiation of treatment. When evaluating treatment results in these 18 patients, we observed patients exhibiting a wide range of therapeutic responses. Included among these were exemplary cases of clinical response to therapy (mixed, partial, or complete), disease progression, hyperprogressive disease (34, 35), and pseudoprogression. Each of these will be discussed as individual case studies below. A summary of the results from all 18 of these patients is included in Table 2.

We utilized the same set of 18 patients to evaluate the PFS of patients classified by either the GIN or RECIST imaging response criteria. However, because 1 patient (Table 2, patient 111) did not show either an increase or decrease in GIN and, therefore, prediction of "response" versus "progression" could not be made, the PFS dataset consists of 17 patients. There was 1 patient (Table 2, patient 110) who was predicted to respond by GIN, but progressed by RECIST; for other patients, GIN prediction and RECIST outcome were concordant. Hence, there were 7 patients predicted to respond and 10 patients predicted to be progressors by GIN; by RECIST, there were 6 responders and 11 progressors. The Kaplan–Meier curve (Fig. 2B) demonstrated that the median PFS for responders versus progressors (as predicted by GIN) was 12.0 [95% confidence interval (CI), 0–25.5 months] versus 2.05 months (95% CI, 1.5–2.3 months). HR (95% CI) for PFS for GIN-predicted progressors versus responders was 5.74 (1.9–17.7; $P = 0.001$). For RECIST, the Kaplan–Meier curve showed a median PFS for responders was not reached after a median follow-up time of 13.4 months (95% CI, 8.3–18.5), whereas for progressors, it was 2.2 months [95% CI, 1.8–2.6 months; HR (95% CI) for RECIST progressors vs. responders = 7.42 (2.47–22.3; $P < 0.001$)]. When classifying patients as either responding or progressing after treatment using the GIN versus RECIST value, the median PFS was 12.0 versus not reached at a median follow-up of 13.4 months for responders; the median PFS was 2.05 versus 2.25 months, respectively, for progressors (GIN vs. RECIST, all P values nonsignificant).

The one discordant patient with GIN prediction of response, but progression by RECIST imaging, showed clonal selection driving the GIN changes

In the 1 patient with discordancy between GIN prediction and RECIST outcome (Table 2, patient 110), a reduction in the GIN at day +28 and through day +56 was observed followed by an increased GIN back to near baseline by day +85 (Supplementary Fig. S4B). The RECIST response showed SD that, however, lasted only 4 months; hence, the patient was considered a progressor. Interestingly, examination of the genome-wide cfDNA profiles revealed that the initial decrease and subsequent increase in the GIN were driven by clonal selection (Supplementary Fig. S4A and S4C). Hence, these data suggest a potential role for clonal selection and expansion as a mechanism of resistance in patients receiving immunotherapy. Clinically, such changes could manifest as stable disease or as a response followed by progression; alternatively, such a phenomenon could present as a mixed response wherein some tumors regress and others grow.

GIN patterns predictive of response

Overall, the use of cfDNA predicted that 7 patients would be responders and, of these, 6 met our criteria for response (SD > 9 months/PR/CR). Figure 3 shows the GIN patterns for all 7 patients. Included among these were the following observations: (i) patient 1 [metastatic basal cell carcinoma with near complete response (PFS, 18+ months; ref. 36)] exhibited an initial increase in GIN, followed by a steep fall by about week 6; (ii) patient 40 [metastatic cutaneous squamous cell carcinoma with CR (PFS, 13.4+ months; Figs. 3 and 4A–C)] showed a high GIN of 4,654 at baseline that increased to a maximum of 5,898 at day +21 before decreasing again at day +42, reaching a level below our limit of detection at day 63 and remaining low at day +339; (iii) patient 51 (ocular melanoma with SD for 12 months) also showed an increase in GIN by day 21, which then decreased by day 63 (no sample was available between days 21 and 63) and stayed low through day 264, but then increased on day 320 (about 6 weeks before imaging showed progression at 12 months); (iv) patient 55 [melanoma with CR (PFS, 10+ months)] did not show the initial spike in GIN, but rather demonstrated a continuous decrease in GIN starting at day 21 and through day 55; (v) patient 114 [squamous cell carcinoma of the lung with PR (PFS, 5.1 months)] showed a slight increase in GIN by day 36 followed by a drop at the next sample collection time point (day 63); (vi) patient 125 [gastroesophageal (GE) junction adenocarcinoma with early pseudoprogression followed by PR (PFS,

Published OnlineFirst February 4, 2019; DOI: 10.1158/1535-7163.MCT-18-0535

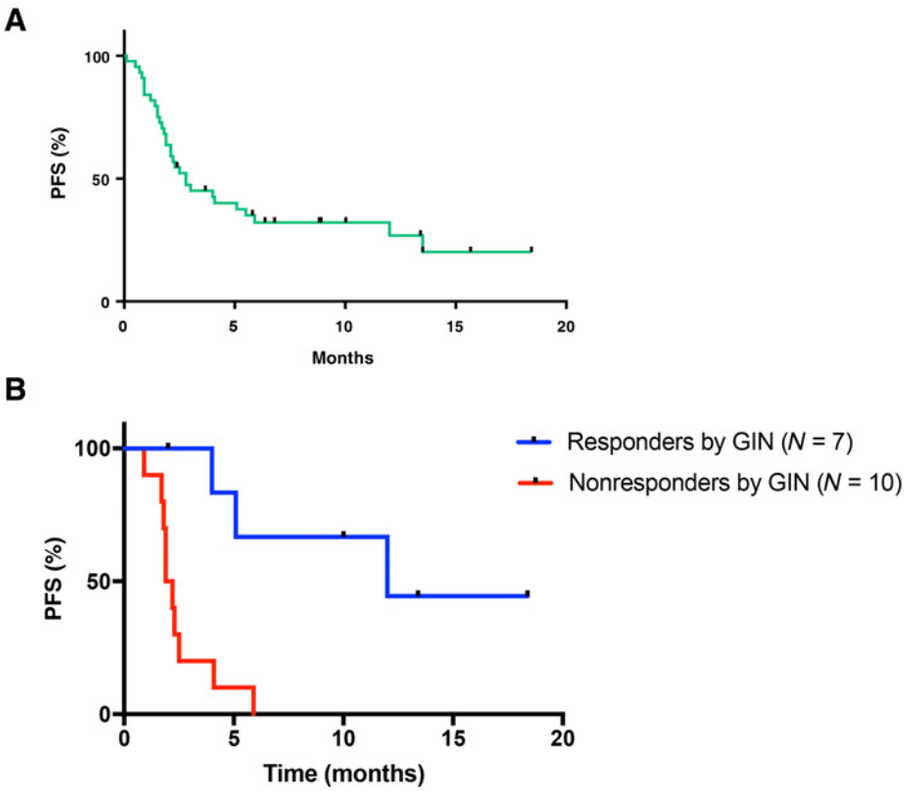

Figure 2.
A, PFS for all 44 patients with sufficient data for analysis. The median PFS (range) was 2.8 (0.1–18.4+) months, calculated using the method of Kaplan and Meier. **B,** Kaplan and Meier PFS for GIN-predicted responders ($N = 7$; blue line) versus nonresponders ($N = 10$; red line). GIN prediction based on cfDNA profiles at approximately 6 weeks compared with baseline. Median PFS for GIN-predicted responders versus nonresponders = 12.0 versus 2.05 months ($P = 0.001$); HR (95% CI) for PFS for GIN-predicted progressors versus responders was 5.74 (1.9–17.7; $P = 0.001$).

Table 2. Patient response and GIN prediction of outcome ($N = 18$)[a]

Patient ID	Diagnosis	Immunotherapy	PFS[b] (months)	Outcome	GIN Prediction[c]	Comments
1	Basal cell carcinoma	Nivolumab	18.43+	Response (PR)	Response	
30	Head and neck SCC	Pembrolizumab	5.9	Progression	Progression	See Fig. 4
40	Cutaneous SCC	Pembrolizumab	13.40+	Response (CR)	Response	See Fig. 4
40B	Bladder urothelial carcinoma	Atezolizumab + SBRT	1.8	Progression	Progression	Hyperprogression; see Fig. 4
51	Ocular melanoma	Nivolumab/ipilimumab	12.0	Response (SD 12 months)	Response	
55	Melanoma	Nivolumab/ipilimumab	10.03+	Response (CR)	Response	
65	Colorectal adenocarcinoma	Nivolumab + SBRT	2.3	Progression	Progression	
67	NSCLC SCC	Nivolumab + SBRT	1.7	Progression	Progression	
69	NSCLC adenocarcinoma	Pembrolizumab	4.1	Progression	Progression	
70	Basal cell carcinoma	Pembrolizumab	2.5	Progression	Progression	
79	Endometrial sarcoma	Nivolumab + vismodegib + trametinib + anastrozole	1.9	Progression	Progression	
82	Thyroid cancer	Pembrolizumab	1.9	Progression	Progression	
83	Ovarian cancer	Nivolumab + SBRT	0.9	Progression	Progression	
100	Neuroendocrine carcinoma of unknown primary	Nivolumab + trametinib	2.2	Progression	Progression	
110	Esophageal cancer	Nivolumab	4.0	Progression	Response	See Supplementary Fig. S4
111	Breast cancer	Pembrolizumab	5.5	Progression (after 5.5 months of SD)	SD	Minimal change in GIN noted at day +43
114	NSCLC SCC	Nivolumab	5.1	Response (PR)	Response	
125	GE junction adenocarcinoma	Pembrolizumab + SBRT	2.0+	Response (PR)	Response	Pseudoprogression; see Fig. 4

Abbreviations: GE junction, gastroesophageal junction; ID, identification number; NSCLC, non–small cell lung cancer; SBRT, stereotactic body radiation therapy; SCC, squamous cell cancer.
[a]Patients with SD $\leq$ 9 months and PD are considered progressors; patients with SD > 9 months/PR/CR are considered responders.
[b]PFS values with a (+) indicate response is ongoing at time of data censoring. Data for GIN prediction taken from day +42 or the nearest time point thereafter.
[c]Patient 110 showed a clonal response by GIN, but achieved only short-lived (4 month) SD (Supplementary Fig. S5); hence, in this patient, the GIN prediction of response was considered discrepant with the RECIST findings and our classification of this individual as a progressor. Patient 111 showed only a marginal change at day +43, and GIN could therefore not be used to predict either response or progression; the patient had SD that lasted 5.5 months, and then the tumor progressed. For Patient 83, data from day +21 were used for GIN prediction due to a change in therapy to chemotherapy soon after that date.

Published OnlineFirst February 4, 2019; DOI: 10.1158/1535-7163.MCT-18-0535

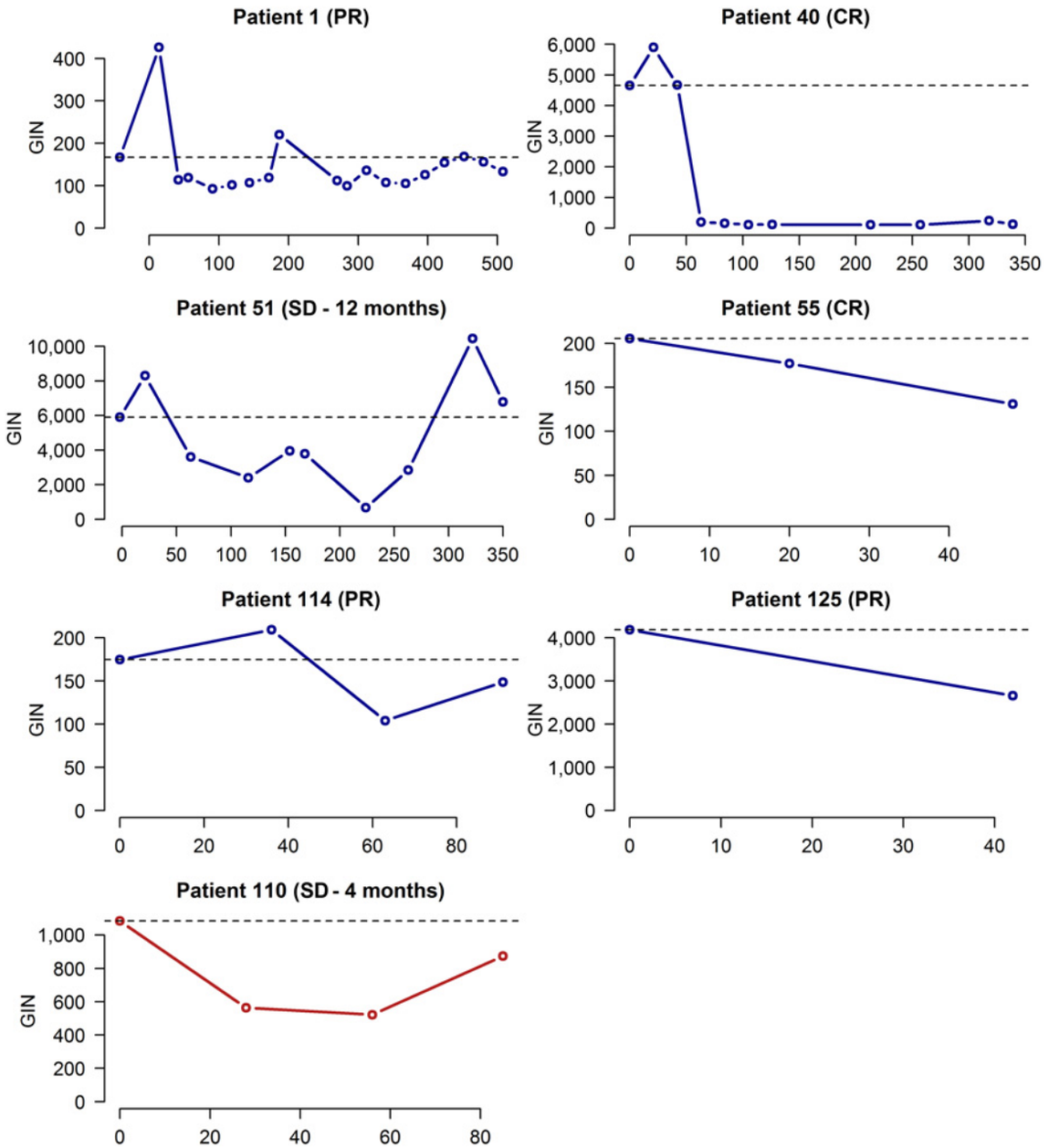

Figure 3.

Examples of GIN profiles of 7 patients predicted to be responders by GIN (responder defined as achieving SD > 9 months, PR or CR). *X* axis, day since start of treatment; *Y* axis, GIN value. Open circles represent measured samples with time relative to the treatment initiation (day 0; *X* axis). Blue profiles = partial or complete remission ($N = 6$ patients; patient numbers 1, 40, 51, 55, 114, and 125; Table 2); red profile = discordant sample (GIN predicted response, whereas clinical showed SD for 4 months and then PD; patient number 110). Black dashed line represents the baseline GIN for each patient. Additional details about patient 110 are included in Supplementary Fig. S4.

2+ months; Fig. 4J–M)] showed a drop in GIN at the first time point (day +43) assessed after starting therapy; and (vii) patient 110 [esophageal cancer (SD for 4 months)] showed a drop in GIN on day 28 lasting through day 56, representing the one discordancy between GIN prediction of response versus actual outcome (Supplementary Fig. S4 and results above show clonal selection accounting for the discrepancy). Taken together, these results demonstrate that patterns of the GIN throughout the early phases of immunotherapy treatment were consistent with response in six of seven cases. Furthermore, the pattern of GIN changes included a rise in GIN in the first few weeks followed by a drop in GIN starting at about day +42 or soon thereafter in four of the five correctly predicted responders who had a sample available for assessment before the 6-week time point.

Published OnlineFirst February 4, 2019; DOI: 10.1158/1535-7163.MCT-18-0535

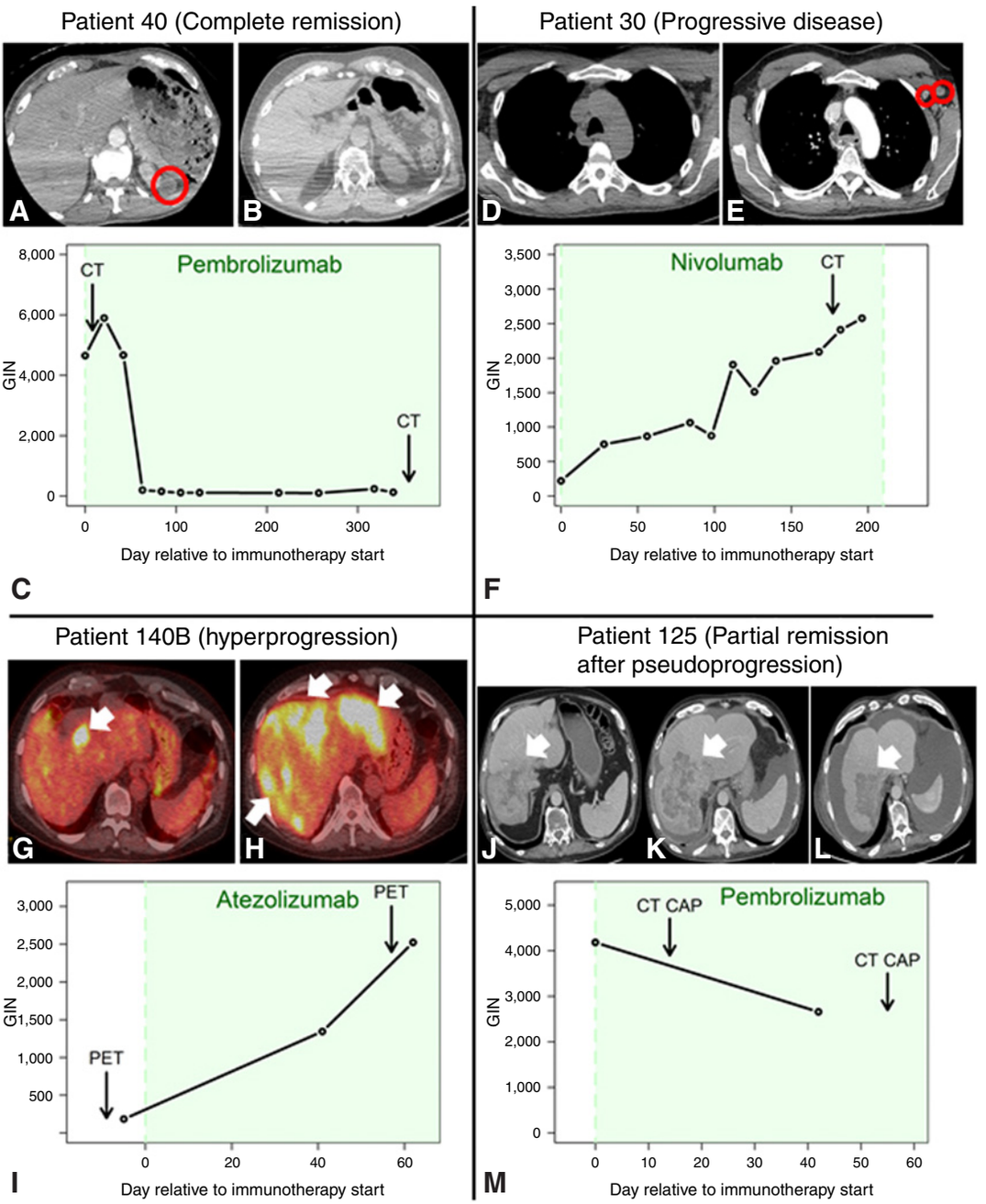

Figure 4.

Representative case studies for distinct clinical responses to immunotherapy. Top, Left**,** Patient 40 demonstrated a clinical response with CT scan from the first scan (**A**) and day +356 (**B**) shown. **C,** GIN for all samples collected across this study for patient 40 shown. Each measured cfDNA sample is indicated by an open circle. Green rectangle is representative of treatment window. Top, Right**,** Patient 30 demonstrated PD with CT scans from the first scan (**D**) and day +177 (**E**) shown. **F,** GIN for all samples collected across this study for patient 30 shown. Each measured cfDNA sample is indicated by an open circle. Green and red rectangles are representative of treatment windows. Bottom, Left**,** Patient 40B demonstrated accelerated progression or hyperprogressive disease (HPD; refs. 35, 36) with PET scans from the initial scan (**G**) and day +57 (**H**) shown. **I,** GIN for all samples collected across this study for patient 40B shown. Each measured cfDNA sample is indicated by an open circle. Green rectangle is representative of treatment window. Bottom, Right**,** Patient 125 demonstrated pseudoprogression with CT scans from the initial scan (**J**), day +14 (**K**), and day +55 (**L**) shown. **M,** GIN for all samples collected across this study for patient 125 shown. Each measured cfDNA sample is indicated by an open circle. Green rectangle is representative of treatment window. Abbreviation: CT CAP, computerized tomographic scan of chest, abdomen, and pelvis.

Published OnlineFirst February 4, 2019; DOI: 10.1158/1535-7163.MCT-18-0535

GIN patterns predictive of progression

There were 11 patients that had GIN values that were unchanged ($N = 1$; Table 1, patient 111) or continued to increase ($N = 10$) throughout treatment with checkpoint inhibitors (Supplementary Fig. S5). All 10 patients with increasing GIN were considered nonresponders/progressors (SD $\leq$ 9 months or PD). An interesting example of disease progression is illustrated in Fig. 4 (patient 30, head and neck squamous cell carcinoma). The GIN for this patient increased continuously from 221 at baseline through week 6 and reaching a peak of 2,578 after 196 days of treatment (Fig. 4F), consistent with the increased tumor burden observed by CT scan on day +177 (Fig. 4D and E). Based upon the consistent increase observed in the GIN, the fact that this patient would not achieve tumor regression or durable SD was predicted by cfDNA weeks before the CT scan showed overt progression (Fig. 4F).

GIN-level pattern in serial samples differentiated hyperprogression from pseudoprogression and pseudoprogression from true progression

In addition to patients whose tumors grew despite treatment with checkpoint inhibitors, recent evidence suggests that a subset of individuals exhibit enhanced tumor growth rates during immunotherapy treatment (34, 35). Furthermore, there is another unusual postimmunotherapy pattern of response called pseudoprogression, which reflects worsening scans in the face of disease that will ultimately regress. Differentiating true accelerated hyperprogression from pseudoprogression and distinguishing pseudoprogression from true progression are crucial for clinical decision-making.

Examples of each of these types of treatment response are depicted in Fig. 4. Patient 40B (Fig. 4G and H) had bladder urothelial carcinoma and demonstrated rapid progression that was eventually deemed hyperprogression (though at the time of PET scans showing dramatic disease flare, it was not clear whether this was pseudoprogression or real progression). This patient had a GIN value of 186 when measured at day –5; however, this value rapidly increased to 1,345 at day +41 before reaching a maximum of 2,525 at day +62 of treatment (Fig. 4I). Using the data from day +41, this is associated with an increase of the GIN at +25.19 units/day. This rapid increase in the GIN is consistent with the hyperprogressive disease diagnosed clinically.

We also observed an instance of pseudoprogression after pembrolizumab therapy. Patient 125 was diagnosed with GE junction adenocarcinoma and began receiving combination treatment with pembrolizumab and stereotactic body radiation therapy (Fig. 4J). After 14 days, a CT scan revealed PD compared with scans done several weeks before starting therapy (Fig. 4K); however, treatment with pembrolizumab continued because the patient reported a reduction in general malaise. The GIN obtained using the cfDNA from this patient showed a decrease from 4,181 at day 0 to 2,658 at day +42 (Fig. 4M). In contrast to patient 40B that showed an increasing GIN over time (+25.19 units/day), patient 125 showed a decrease in the GIN rate over time of –36.26 units/day. This reduction in GIN over time would be consistent with a response to treatment rather than disease progression. A CT scan was again performed on day +55 and showed a partial remission (Fig. 4L). These data are consistent with the cfDNA correctly identifying that this patient likely exhibited pseudoprogression at the time of initial imaging, and the GIN was consistent with the observed PR.

Discussion

Modulation of members of the immune checkpoint pathway using therapeutic antibodies has changed cancer medicine and resulted in some patients exhibiting long-lasting, robust responses; however, clinical response is not observed in the majority of patients, some individuals suffer from significant side effects and recent reports indicate that these drugs may actually increase tumor growth rate in a subset of patients (34, 35).

When monitoring mutated cfDNA in patients responding to therapies targeted to specific mutations such as those in EGFR, it has been previously described that there is an abrupt increase in cfDNA in the first 2 to 4 days followed by a rapid metabolic clearance (37). We therefore wanted to determine whether immunotherapy treatment resulted in a similar pattern or if the response kinetics for these drugs was distinct. We evaluated the temporal pattern of the GIN in patients that showed a clinical response to immunotherapy and had CNAs that made their profiles evaluable using this method. Six of 18 patients with serial samples showed a response (SD > 9 months/PR/CR) after immunotherapy. GIN patterns after treatment correctly predicted responsiveness in all 6 patients. The specific dynamic patterns observed in responders included GIN levels that continuously decreased or, more commonly, a spike in GIN levels followed by a decrease at about week 6 or soon thereafter (Fig. 3). Eleven patients (deemed progressors) failed to respond (i.e., had SD $\leq$ 9 months or PD) after immunotherapy. GIN predicted progression in 10 of these patients; in 1 patient, GIN predicted response, but the patient only achieved SD for 4 months followed by tumor growth. Close and deep interrogation of the CNAs from this patient revealed clonal selection, i.e., a clone that decreased followed by, at the 2-month landmark, increasing levels of a subclone, hence explaining the discordant results between GIN prediction and actual outcome. Such observations may be helpful in further illuminating underlying disease biological impact after immunotherapy. One additional patient showed stable GIN levels at 6 weeks and, therefore, prediction of response or progression were not possible. Overall concordance between GIN-predicted response and actual outcome was 94% in the 17 patients in whom serial GIN levels could be used to predict response. Importantly, although the response profile frequently seen (initial increase in cfDNA followed by a drop) is consistent with that previously reported in patients treated with molecularly targeted therapeutics, the timeframe is greatly expanded, with the peak and fall occurring within days after EGFR inhibitor administration (37), but over about 6 weeks with the checkpoint inhibitors, suggesting slower kinetic response to immunotherapy relative to targeted therapies.

Because there are no reliable methods for identification of pseudoprogression, the case that was correctly identified using our cfDNA method, as reflected by decreasing GIN levels in the face of an early increase in tumor size on imaging, may be of particular interest (Fig. 4, patient 125); the patient later achieved a PR. This single case study, provided that the results are replicated in future studies, may have utility because the phenomenon of pseudoprogression is a particular challenge to physicians treating

Published OnlineFirst February 4, 2019; DOI: 10.1158/1535-7163.MCT-18-0535

patients with these drugs because it may lead to the early discontinuation of an effective therapy (38).

Hyperprogression is another recently described phenomenon (34, 35). It is defined by time-to-treatment failure <2 months, >50% increase in tumor burden compared with preimmunotherapy imaging, and >2-fold increase in progression pace (35). Patient 40B (Fig. 4) was seen in our clinics (authors S. Kato and R. Kurzrock) and, at the time that the PET scan showed significant worsening, the dilemma of whether this was a sign of rapid progression or represented pseudoprogression (with the increase in metabolic activity on PET scan reflecting immune infiltrate into the tumor that would be followed by a response) was debated extensively. Importantly, the former would mandate immediate drug discontinuation, whereas the latter would suggest continuation of the checkpoint inhibitor. cfDNA showed a rapid and sustained increase in GIN levels consistent with hyperprogression. Although this result was observed in a single patient and thus care should be taken to not overstate these results, continued observation of this association [patient 40B had a GIN value that increased at a rate of +25.19 units per day, as compared with the rate observed in a patient with pseudoprogression (patient 125; −36.26 units/day)] could inform decision-making in similar cases in the future. Importantly, the evaluation of additional patients beyond this cohort is needed to validate these observations.

Performing low-coverage, genome-wide sequencing of cfDNA has benefits relative to high-depth sequencing of targeted panels. When compared with hybridization capture methods, the workflow is simpler and requires less sequencing, thereby decreasing the cost and time required to perform the assay. The workflow of amplification-based methods is relatively efficient, although the sensitivity of such methods is limited by the requirement for opposing primers, which decreases the number of available target molecules that can be amplified from cfDNA in a size-dependent manner. Although there are benefits for the method described herein, there are also limitations to both the method and the sample cohort. First, tumors can be driven not only by CNAs, but also by fusions and point mutations, and the relative proportion of tumors driven by CNAs relative to other mutation types varies by tissue of origin (1). This assay cannot readily detect alternative mutational classes. Second, not all patients will harbor a sufficient amount of cfDNA in the plasma to detect CNAs. The limit of detection for this assay is driven by a number of factors including the size of the CNA, the magnitude of the copy-number change, the tumor DNA fraction, and the depth of sequencing used. At the level of sequencing performed in this study, the limit of detection is likely to be similar to that described for NIPT for an individual CNA (∼2%–4% tumor fraction). It is also worth noting that the CNAs detected using this method are possibly the result of a large number of genomic rearrangements; however, at the sequencing depth used, we cannot delineate the mechanism by which the observed CNAs are formed. Finally, the sample cohort used in this study is small, and thus additional studies will be required to confirm the observed results. Due to both the advantages and limitations of this assay relative to traditional liquid biopsy methods like CTC enumeration, protein biomarkers, and targeted cfDNA deep sequencing, additional studies are warranted to further understand the clinical utility. It is perhaps most likely that this method will provide additional, complimentary information to these more established methods. To address these limitations and identify potential clinical utility, we hope to expand the sample cohort over time.

In summary, the evaluation of the kinetic trajectory of aneuploidy and/or the cancer-specific burden in cfDNA, as reflected by the GIN, can serve as an early indicator of checkpoint inhibitor response versus progression. We did not, however, see a significant correlation between pretherapeutic GIN or cfDNA level and response to immunotherapy, an observation consistent with the report of Weiss and colleagues (11). In contrast, baseline tissue or ctDNA mutational burden can be useful in differentiating a subset of patients with a higher chance of response to checkpoint blockade (39, 40). Of interest, we found that the dynamic response of the tumor to immune checkpoint inhibitors, as measured using cfDNA, is distinct from the kinetics observed in response to therapeutics targeting specific molecular alterations (37). In those patients who ultimately showed a clinical response to checkpoint blockade, it took 3 to 8 weeks for the GIN to decline below the patient-specific baseline level, as compared with about 5 days for targeted therapies. For the patients in our study, blood samples were not collected earlier than 2 weeks following the initiation of treatment; therefore, we cannot conclude definitively what the GIN levels look like in the first 14 days, though responders most commonly showed a spike in GIN levels in the sample collected on or shortly after week 2. Still, future studies are needed to determine the frequency and timing of sample collection to construct a more detailed timeline of the response pattern to checkpoint inhibitors as measured by cfDNA profiling. Our data also suggest that dynamic changes in GIN levels can predate progression or response as ascertained by imaging, and that the GIN pattern may also be exploitable to differentiate hyperprogression from pseudoprogression and pseudoprogression from progression. We chose to use the GIN measurement taken at approximately 6 weeks after the initiation of treatment to retrospectively predict response for this proof-of-concept study; however, additional work is needed to determine the best time during treatment to perform these analyses. Taken together, these data demonstrate a proof of concept for the use of low-coverage, genome-wide sequencing of cfDNA from patients with cancer as a method for monitoring treatment response to immunotherapy.

Disclosure of Potential Conflicts of Interest

A.M. Goodman is a consultant for Defined Health, Jazz Pharma, Tanabe, and Tempus, and received honoraria from the speakers' bureau of Seattle Genetics. G. McLennan has an ownership interest (including stock, patents, etc.) in LabCorp. D.S. Grosu is Chief Medical Officer at, and has an ownership interest (including stock, patents, etc.) in, Sequenom, Inc; he is also a consultant/advisory board member for LabCorp, Inc. M. Ehrich is Founder of JunoDx. R. Kurzrock has an ownership interest in CureMatch, Inc.; reports receiving commercial research grant from Incyte, Genentech, Merck Serono, Pfizer, Sequenom, Foundation Medicine, Guardant Health, and Konica Minolta; received honoraria from the speakers' bureau of Roche; has an ownership interest (including stock, patents, etc.) in CureMatch, Inc., and IDbyDNA; and is a consultant/advisory board member for LOXO, XBiotech, Actuate Therapeutics, Roche, and NeoMed. No potential conflicts of interests were disclosed by the other authors.

Authors' Contributions

Conception and design: T.J. Jensen, A.M. Goodman, C.K. Ellison, P. Nakashe, A.R. Mazloom, G. McLennan, D.S. Grosu, R. Kurzrock

Development of methodology: T.J. Jensen, C.K. Ellison, P. Nakashe, A.R. Mazloom, M. Ehrich
Acquisition of data (provided animals, acquired and managed patients, provided facilities, etc.): T.J. Jensen, A.M. Goodman, S. Kato, G.A. Daniels, L. Kim, P. Nakashe, E. McCarthy
Analysis and interpretation of data (e.-g., statistical analysis, biostatistics, computational analysis): T.J. Jensen, A.M. Goodman, C.K. Ellison, P. Nakashe, A.R. Mazloom, R. Kurzrock
Writing, review, and/or revision of the manuscript: T.J. Jensen, A.M. Goodman, S. Kato, C.K. Ellison, G. Daniels, G. McLennan, D.S. Grosu, M. Ehrich, R. Kurzrock
Administrative, technical, or material support (i.e., reporting or organizing data, constructing databases): T.J. Jensen, C.K. Ellison, E. McCarthy, G. McLennan
Study supervision: T.J. Jensen

Acknowledgments

The authors would like to thank Nian Liu and Xiaojun Guan for data processing and Kai Treuner, Nathan Faulkner, Michael Salmans, David Wong, and Vach Angkachatchai for study coordination and sample processing. This study was supported in part by the Joan and Irwin Jacobs fund, NCI grant P30 CA016672 (R. Kurzrock), and Sequenom, Inc.

The costs of publication of this article were defrayed in part by the payment of page charges. This article must therefore be hereby marked *advertisement* in accordance with 18 U.S.C. Section 1734 solely to indicate this fact.

Received May 17, 2018; revised September 5, 2018; accepted November 26, 2018; published first December 6, 2018.

References

1. Ciriello G, Miller ML, Aksoy BA, Senbabaoglu Y, Schultz N, Sander C. Emerging landscape of oncogenic signatures across human cancers. Nat Genet 2013;45:1127–33.
2. Wood LD, Parsons DW, Jones S, Lin J, Sjoblom T, Leary RJ, et al. The genomic landscapes of human breast and colorectal cancers. Science 2007;318:1108–13.
3. Millis SZ, Ikeda S, Reddy S, Gatalica Z, Kurzrock R. Landscape of phosphatidylinositol-3-kinase pathway alterations across 19784 diverse solid tumors. JAMA Oncol 2016;2:1565–73.
4. Hoadley KA, Yau C, Wolf DM, Cherniack AD, Tamborero D, Ng S, et al. Multiplatform analysis of 12 cancer types reveals molecular classification within and across tissues of origin. Cell 2014;158:929–44.
5. Zack TI, Schumacher SE, Carter SL, Cherniack AD, Saksena G, Tabak B, et al. Pan-cancer patterns of somatic copy number alteration. Nat Genet 2013;45:1134–40.
6. Bettegowda C, Sausen M, Leary RJ, Kinde I, Wang Y, Agrawal N, et al. Detection of circulating tumor DNA in early- and late-stage human malignancies. Sci Transl Med 2014;6:224ra24.
7. Leon SA, Shapiro B, Sklaroff DM, Yaros MJ. Free DNA in the serum of cancer patients and the effect of therapy. Cancer Res 1977;37:646–50.
8. Schwaederle M, Husain H, Fanta PT, Piccioni DE, Kesari S, Schwab RB, et al. Detection rate of actionable mutations in diverse cancers using a biopsy-free (blood) circulating tumor cell DNA assay. Oncotarget 2016;7:9707–17.
9. Tie J, Wang Y, Tomasetti C, Li L, Springer S, Kinde I, et al. Circulating tumor DNA analysis detects minimal residual disease and predicts recurrence in patients with stage II colon cancer. Sci Transl Med 2016;8:346ra92.
10. Schwaederle MC, Patel SP, Husain H, Ikeda M, Lanman RB, Banks KC, et al. Utility of genomic assessment of blood-derived circulating tumor DNA (ctDNA) in patients with advanced lung adenocarcinoma. Clin Cancer Res 2017;23:5101–11.
11. Weiss GJ, Beck J, Braun DP, Bornemann-Kolatzki K, Barilla H, Cubello R, et al. Tumor cell-free DNA copy number instability predicts therapeutic response to immunotherapy. Clin Cancer Res 2017;23:5074–81.
12. Kuziora M, Higgs BW, Brohawn PZ, Raja R, Bais C, Ranade K. Association of early reduction in circulating tumor DNA (ctDNA) with improved progression-free survival (PFS) and overall survival (OS) of patients (pts) with urothelial bladder cancer (UBC) treated with durvalumab (D). J Clin Oncol 2017;35(15 suppl):11538.
13. Janku F, Zhang S, Waters J, Liu L, Huang HJ, Subbiah V, et al. Development and validation of an ultradeep next-generation sequencing assay for testing of plasma cell-free DNA from patients with advanced cancer. Clin Cancer Res 2017;23:5648–56.
14. Husain H, Velculescu VE. Cancer DNA in the circulation: the liquid biopsy. JAMA 2017;318:1272–4.
15. Li M, Diehl F, Dressman D, Vogelstein B, Kinzler KW. BEAMing up for detection and quantification of rare sequence variants. Nat Methods 2006;3:95–7.
16. Newman AM, Bratman SV, To J, Wynne JF, Eclov NC, Modlin LA, et al. An ultrasensitive method for quantitating circulating tumor DNA with broad patient coverage. Nat Med 2014;20:548–54.
17. Ehrich M, Tynan J, Mazloom A, Almasri E, McCullough R, Boomer T, et al. Genome-wide cfDNA screening: clinical laboratory experience with the first 10,000 cases. Genet Med 2017;19:1332–7.
18. McCullough RM, Almasri EA, Guan X, Geis JA, Hicks SC, Mazloom AR, et al. Non-invasive prenatal chromosomal aneuploidy testing–clinical experience: 100,000 clinical samples. PLoS One 2014;9:e109173.
19. Ehrich M, Deciu C, Zwiefelhofer T, Tynan JA, Cagasan L, Tim R, et al. Noninvasive detection of fetal trisomy 21 by sequencing of DNA in maternal blood: a study in a clinical setting. Am J Obstet Gynecol 2011;204:205e1–11.
20. Jensen TJ, Zwiefelhofer T, Tim RC, Dzakula Z, Kim SK, Mazloom AR, et al. High-throughput massively parallel sequencing for fetal aneuploidy detection from maternal plasma. PLoS One 2013;8:e57381.
21. Palomaki GE, Kloza EM, Lambert-Messerlian GM, Haddow JE, Neveux LM, Ehrich M, et al. DNA sequencing of maternal plasma to detect Down syndrome: an international clinical validation study. Genet Med 2011;13:913–20.
22. Bianchi DW, Chudova D, Sehnert AJ, Bhatt S, Murray K, Prosen TL, et al. Noninvasive prenatal testing and incidental detection of occult maternal malignancies. JAMA 2015;314:162–9.
23. Dharajiya NG, Grosu DS, Farkas DH, McCullough RM, Almasri E, Sun Y, et al. Incidental detection of maternal neoplasia in noninvasive prenatal testing. Clin Chem 2018;64:329–35.
24. Patel SP, Kurzrock R. PD-L1 expression as a predictive biomarker in cancer immunotherapy. Mol Cancer Ther 2015;14:847–56.
25. Rizvi NA, Hellmann MD, Snyder A, Kvistborg P, Makarov V, Havel JJ, et al. Cancer immunology. Mutational landscape determines sensitivity to PD-1 blockade in non-small cell lung cancer. Science 2015;348:124–8.
26. Davoli T, Uno H, Wooten EC, Elledge SJ. Tumor aneuploidy correlates with markers of immune evasion and with reduced response to immunotherapy. Science 2017;355.
27. Roh W, Chen PL, Reuben A, Spencer CN, Prieto PA, Miller JP, et al. Integrated molecular analysis of tumor biopsies on sequential CTLA-4 and PD-1 blockade reveals markers of response and resistance. Sci Transl Med 2017;9.
28. Eisenhauer EA, Therasse P, Bogaerts J, Schwartz LH, Sargent D, Ford R, et al. New response evaluation criteria in solid tumours: revised RECIST guideline (version 1.1). Eur J Cancer 2009;45:228–47.
29. Ellison CK, Sun Y, Hogg G, Fox J, Tao H, McCarthy E, et al. Using targeted sequencing of paralogous sequences for noninvasive detection of selected fetal aneuploidies. Clin Chem 2016;62:1621–9.
30. Tynan JA, Kim SK, Mazloom AR, Zhao C, McLennan G, Tim R, et al. Application of risk score analysis to low-coverage whole genome sequencing data for the noninvasive detection of trisomy 21, trisomy 18, and trisomy 13. Prenat Diagn 2016;36:56–62.
31. Lefkowitz RB, Tynan JA, Liu T, Wu Y, Mazloom AR, Almasri E, et al. Clinical validation of a noninvasive prenatal test for genomewide detection of fetal copy number variants. Am J Obstet Gynecol 2016;215:227e1–e16.
32. Zhao C, Tynan J, Ehrich M, Hannum G, McCullough R, Saldivar JS, et al. Detection of fetal subchromosomal abnormalities by sequencing circulating cell-free DNA from maternal plasma. Clin Chem 2015;61:608–16.

Published OnlineFirst February 4, 2019; DOI: 10.1158/1535-7163.MCT-18-0535

33. Team RDC. R: a language and environment for statistical computing. Vienna, Austria: R Foundation for Statistical Computing; 2008.
34. Champiat S, Dercle L, Ammari S, Massard C, Hollebecque A, Postel-Vinay S, et al. Hyperprogressive disease is a new pattern of progression in cancer patients treated by anti-PD-1/PD-L1. Clin Cancer Res 2017; 23:1920–8.
35. Kato S, Goodman A, Walavalkar V, Barkauskas DA, Sharabi A, Kurzrock R. Hyperprogressors after immunotherapy: analysis of genomic alterations associated with accelerated growth rate. Clin Cancer Res 2017;23: 4242–50.
36. Ikeda S, Goodman AM, Cohen PR, Jensen TJ, Ellison CK, Frampton G, et al. Metastatic basal cell carcinoma with amplification of PD-L1: exceptional response to anti-PD1 therapy. NPJ Genom Med 2016;1.
37. Husain H, Melnikova VO, Kosco K, Woodward B, More S, Pingle SC, et al. Monitoring daily dynamics of early tumor response to targeted therapy by detecting circulating tumor DNA in urine. Clin Cancer Res 2017;23:4716–23.
38. Chiou VL, Burotto M. Pseudoprogression and immune-related response in solid tumors. J Clin Oncol 2015;33:3541–3.
39. Goodman AM, Kato S, Bazhenova L, Patel SP, Frampton GM, Miller V, et al. Tumor mutational burden as an independent predictor of response to immunotherapy in diverse cancers. Mol Cancer Ther 2017;16:2598–608.
40. Khagi Y, Goodman AM, Daniels GA, Patel SP, Sacco AG, Randall JM, et al. Hypermutated circulating tumor DNA: correlation with response to checkpoint inhibitor-based immunotherapy. Clin Cancer Res 2017; 23:5729–36.

Published OnlineFirst February 4, 2019; DOI: 10.1158/1535-7163.MCT-18-0535

Molecular Cancer Therapeutics

Genome-Wide Sequencing of Cell-Free DNA Identifies Copy-Number Alterations That Can Be Used for Monitoring Response to Immunotherapy in Cancer Patients

Taylor J. Jensen, Aaron M. Goodman, Shumei Kato, et al.

Mol Cancer Ther 2019;18:448-458. Published OnlineFirst February 4, 2019.